Organic & Supramolecular Chemistry

Chiral Polyurea from Tartaric Acid Derived and Lysine Backbone: A Synthetic and Computational Study

Gizem Çalışgan Ünay,[a] Erol Yıldırım,[a, b] and Akin Akdag*[a, b]

In recent years, the studies on artificial helical polymers have become an attractive field due to their impressive optical activity and functions. They have numerous potential applications in many areas such as chiral recognition, enantioselective crystallization, enantioselective release, asymmetric catalysis, and 3D displays.Two new urea containing polymers were synthesized in this study. **P-1** synthesis was accomplished, starting from tartaric acid. Tartaric acid was successfully converted to diamine **4**. The diamine was treated with a *p*-phenylene diisocyanate to get helical structures at the macroscopic level, as evidenced by SEM images. This was shown to be the case through interchain H-bonding between urea groups and microphase separation between the segments due to hydrophobicity difference along the chain. Limited conformational space in **P-1** also assisted the helical structure formation. **P-2** was synthesized by treating *L*-lysine with *p*-phenylene diisocyanate. Due to the ample conformational space and intersegmental mixing due to hydrogen bond between urea and *L*-lysine segments, **P-2** was shown not to be in a helical conformation. Molecular dynamics simulations and first principle studies were used to explain observed structural behaviour for these polymers.

Introduction

The helical structure is one of the most outstanding motifs that is encountered at various scales. From molecular level to the macroscopic level, these structures frequently occur in nature such as α-helices in proteins, DNA double helix molecular level, helical vessels, bacterial flagella on the microscopic level, and seed pods, plant tendrils on the macroscopic level.[1–5] In such systems, the helix structure is critical for their biological functions.[6] Small chiral building blocks arrange themselves into a helical structure due to intramolecular interactions and external factors like solvation.[7–9]

[a] G. Ç. Ünay, E. Yıldırım, A. Akdag
Department of Chemistry, Middle East Technical University, Ankara 06800, Turkey
Tel.: +90 (312) 210 3236
E-mail: aakdag@metu.edu.tr
[b] E. Yıldırım, A. Akdag
Department of Polymer Science and Technology, Middle East Technical University, Ankara, Turkey

Supporting information for this article is available on the WWW under https://doi.org/10.1002/slct.202003534

In recent years, the studies on artificial helical polymers have become an attractive field due to their impressive optical activity and functions.[10–15] They have numerous potential applications in many areas such as chiral recognition, enantioselective crystallization, enantioselective release, asymmetric catalysis, and 3D displays.[16–19]

The history of synthetic helical polymers started with the synthesis of highly isotactic polypropylene (**R1**), which showed a helical structure in its crystalline state in the 1950s by Natta.[20] Although the polymer was a mixture of both left and right-handed helices in the solid-state and the helical structure could not be preserved in solution, this study was a remarkable landmark in this field. After Natta's discovery, Pino,[21] Nolte[22] (**R2**), Okamato[23] (**R3**), Vogl[24] (**R4**), Green[25] (**R5**) (Figure 1), and others have taken the research on this area one step further by adapting helical conformation in solution.

The current synthetic helical polymers maintaining their helical conformation in a solution can be categorized in two classes according to their helix inversion barrier; static and dynamic helical polymers (Figure 2).[26]

The static helical polymers consist of either right or left-handed helix. The interconversion has a significantly high inversion barrier. Thus either handed helices are stable at room temperature. In theory, these types of polymers can be synthesized either from optically active monomers or achiral monomers.[27] Although the former case is not proven in literature at the macromolecular level, there exist examples for oligomeric structures.[28] In the case of achiral monomer, a helix sense polymerization method is applied. In this method, macromolecular static helicity is provided by a chiral catalyst or an initiator. Due to the steric repulsion of the bulky groups on the side chains, the preferred helix conformation is locked throughout the polymerization. This furnished helicity to the polymers. Such processes occur under kinetic control.[26]

Besides the static helical polymers, alternative structure, namely dynamic helical polymers, has been uncovered in the late 1980s.[25] These types of polymer chains contain left and right-handed helices equal in solution; these helices are converted into a full sense polymer upon addition of a chiral entity due to the low helix inversion barrier.[29,30] In other words, the left and right-handed helical parts of the polymer chain can interconvert their conformation to one conformation. These interconversions are called conformational changes; however, the changes create a new configuration (P and M) on the polymer. Therefore these changes should be called conformational configuration change. Chiral pendant groups covalently bonded to the polymer backbone determine the conformation

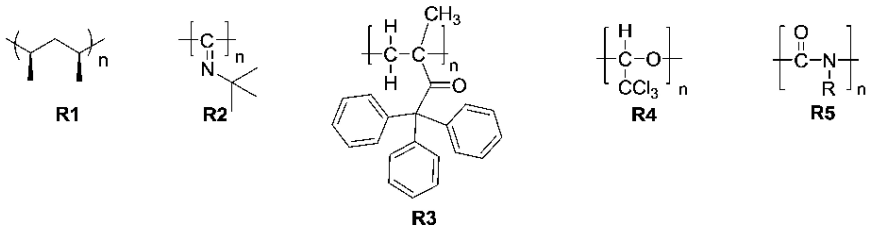

Figure 1. Structures of helical polymers synthesized by Natta (R1), Nolte (R2), Okamato (R3), Vogl (R4) and Green (R5).

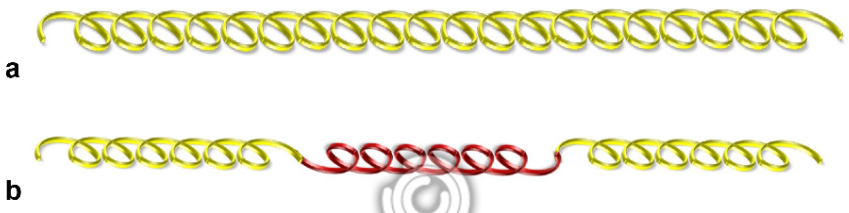

Figure 2. Types of a polymer according to their helix inversion barrier. a) Static helical polymer with high helix inversion barrier. b) Dynamic helical polymer with low helix inversion barrier.

of the dynamic helical polymers. The helicity of these types of polymers is regulated under thermodynamic control.[31]

For the synthesis of chiral helical polymers, chirality has generally been introduced to structure with the help of chiral side chains, chiral initiator, or specific reaction conditions.[32] To the best of our knowledge, synthetic helical polymers having a chiral backbone have not been synthesized. Yet, Isosorbide- and isomannide-based polyurethanes and isocyanopeptides were reported to be helical.[33,34] Up to know, the chiral backbone concept was mostly applied in the field of supramolecular chemistry.[35–37] Besides, there are considerable studies in the field of helically controlled peptidomimetics.[38–40] In this study, we proposed that the main chain helical conformational configuration can be controlled by the use of chiral monomers on the backbone. With this in mind, tartaric acid and lysine were modified to be the backbone of a chiral polymer (Figure 3). These chiral repeating units would be joined together with *p*-phenylene diisocyanate to have urea containing chiral polymers. To further prove our proposal, classical molecular mechanics and first principle calculations were performed to elucidate observed chain behaviours.

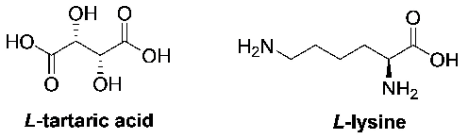

Figure 3. The chiral starting material used as a starting material.

Computational Methods

Two different classical calculations were performed to explain observed experimental structures. Conformational analysis were carried out as a first method on the monomers of **P-1** and **P-2**. Phenyl groups were used as terminal groups on both sides of monomers to avoid urea end group effects (Figure 4a–4b). Number of rotatable torsional angles were determined as 10 for the **P-1** monomer and 13 for the **P-2** monomer. Stochastic searches that involve random perturbations of monomer conformations were used to explore conformational space, since these methods are more appropriate than computationally expensive systematic angle search. It was previously determined that stochastic searches can span conformational space successfully and produces low energy conformations for monomers.[41] 250,000 different conformers were evaluated to obtain a reasonable sampling of the low energy conformations where energies were calculated by using COMPASS force field.[42]

Hexamers based on the calculated lowest energy conformers in the first step are given in Figure 4c–4d for **P-1** and Figure 4e for **P-2**. These were constructed and minimized by molecular mechanics methods. Both structures maintain their structures calculated by conformational analysis. Next, electrostatic potential surface were calculated for these optimized structures by using B3LYP functional[43–45] and 6-311 g(d) basis set as implemented in Gaussian09 software.[46]

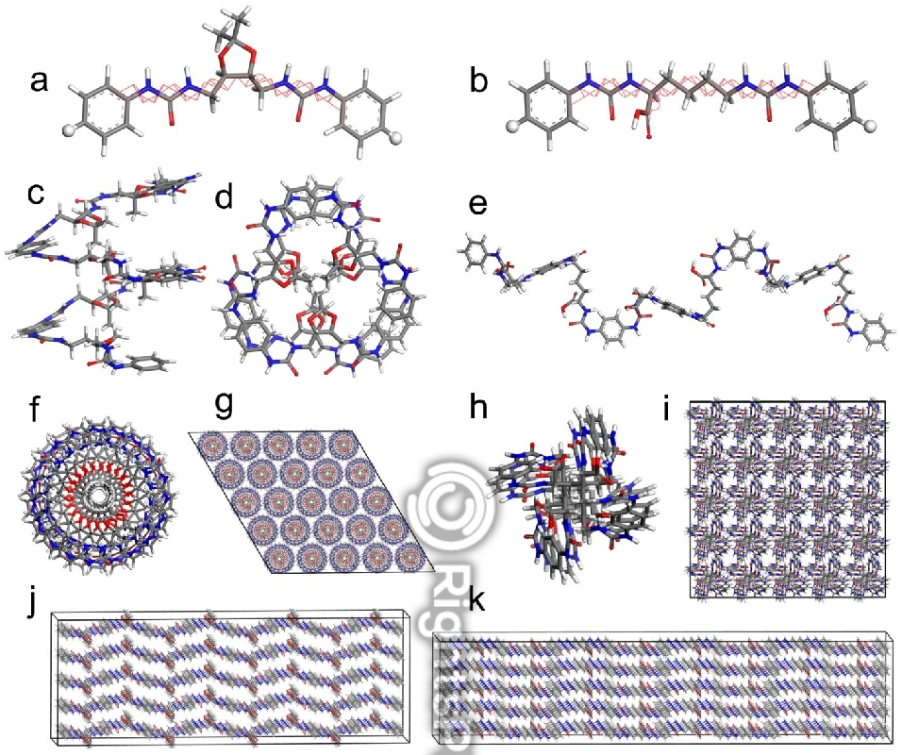

Figure 4. (a) Torsions on monomers of **P-1** and (b) **P-2** with phenyl end groups modelled for conformational analysis, (c)side view and (d) top view hexamers of **P-1**, (e) **P-2** based on the lowest energy conformers calculated at the first step, (f) Octamers of **P-1** and (h) **P-2**, (g) 5×5 supercell of these octamers for **P-1**, (i) **P-2** based on lowest energy conformers constructed under periodic boundary conditions, (j) 5×5 supercell of linear minimized octamer chains constructed manually under periodic boundary conditions for **P-1**, (k) 5×5 supercell of linear minimized octamer chains constructed manually under periodic boundary conditions for **P-2**.

Octamers of the lowest energy conformers were prepared by maintaining the calculated torsional angles constant, and 5×5 supercell were constructed for these chains under periodic boundary conditions given in Figure 4f-4 g for **P-1** and Figure 4h-4i for **P-2**.

In the second classical simulation method, linear minimized octamer chains were build manually, and 5×5 supercell were constructed for these chains under periodic boundary conditions as given in Figure 4j for **P-1** and Figure 4k for **P-2**. The cells prepared by using these linear chains were set to have lower cell density at 0.5 g/cc. Molecular dynamics simulations at room temperature were performed under NVT ensemble during 3 ns with 1 fs steps where trajectory saved at every 30000 steps, where each saved trajectory by the simulation was also minimized without any constraint on lattice parameters to increase cell density slowly at every trajectory. 12.5 Å cut off distance was treated for Van der Waals interactions and particles-mesh (PPPM) summation was used for nonbond electrostatic interactions with 10^{-4} kcal/mol accuracy. Molecular mechanics minimizations and molecular dynamics simulations were conducted by using LAMMPS software.[47] Discovery Studio Visualizer[48] and VMD[49] software were used for visualization and analysis. Octanol/water partition coefficient values (logP) were calculated to quantify the hydrophobicity of monomers and functional units of **P-1** and **P-2** by using Molinspiration software based on group contributions method.[50]

Results and Discussion

Due to the exciting properties of helical polymers from a material science point of view, they received our attention. Furthermore, urea containing helical polymers could be used for asymmetric reactions.[51–54] There are numerous studies that use chiral urea derivatives for asymmetric synthesis. With all these in mind, having chiral polymeric urea units would help

the asymmetric synthesis advanced further. We designed two polymers that would have a helical configuration that either incorporates lysine or tartaric acid derived diamine together with a *p*-phenylene diisocyanate to form urea units. A simple MM2 calculation on oligomeric structures revealed that the designed polymers would have a helical configuration (Figure 5).

For the synthesis of **P-1**, *L*-tartaric acid was subjected to esterification with methanol in the presence of thionyl chloride. Compound **1** was obtained with a 93% yield. The diol **1** was protected with 2,2-dimethoxypropane to get **2** with an 82% yield. For the synthesis of diamine, several methods were employed, and the best yields were obtained with the method shown in Scheme 1 (see *Supporting Information for experimental details*). The fully protected tartaric acid **2**, was treated with ammonia at −40 °C in methanol in a closed vessel. The resulting mixture was heated to 50 °C for 6 hours. Subsequently, the target compound **3** was obtained as a solid with a 91% yield. The amide **3** was reduced to the corresponding diamine **4** with $LiAlH_4$.

p-Phenylene diisocyanate was synthesized from *p*-phenylene diamine and triphosgene under reflux conditions in toluene (Scheme 2). The reaction was complete after the HCl release ceased. After filtration of reaction mixture, the filtrate was evaporated to give *p*-phenylene diisocyanate as a solid.

p-Phenylene diisocyanate (**5**) in anhydrous DMF was added to diamine **4** in DMF. The target polymer was isolated after pouring the mixture into the water. The polymer **P-1** was not soluble in common organic solvents, including DMSO. The characterization of the polymer was accomplished with solid-state ^{13}C NMR. The NMR results showed that in the region between 5–15 ppm **a** carbons, 15–75 ppm **c** and **d**, 85–95 ppm **b** carbons appear. Aromatic carbons were in the region between 95–150 ppm. At around 160 ppm urea carbon peaks were observed (Figure 6).

The DSC measurements showed an endothermic peak at 82.05 °C. The heating was continued to 250 °C and cooled down. No exothermic peaks were observed. This showed that the compound decomposed at 250 °C. This was further checked by the melting point apparatus that there was also no melting, yet the compound started to decompose beyond 200 °C. IR spectrum of the polymer also showed the formation of urea functionality with peaks at 1648 cm^{-1} and 3313 cm^{-1}

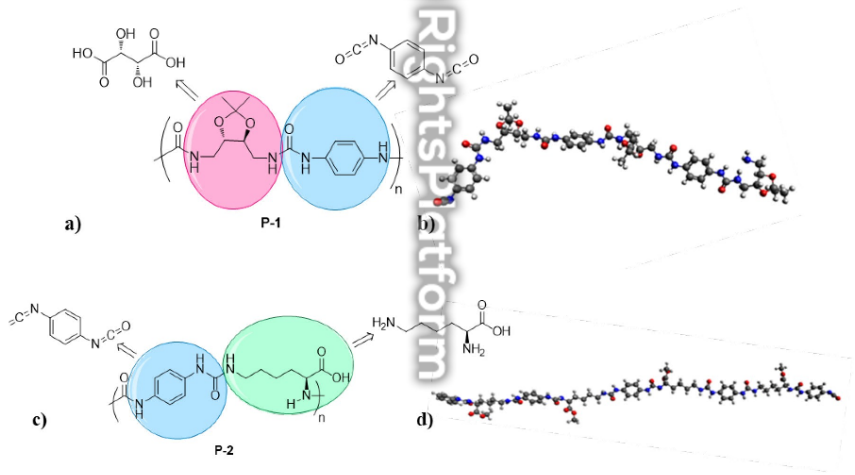

Figure 5. a) retrosynthesis of P-1 b) structure of P-1 obtained from MM2 calculation c) retrosynthesis of P-2 d) structure of P-2 obtained from MM2 calculation.

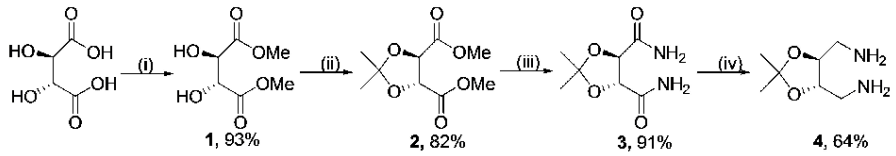

Scheme 1. Reagents and conditions: (i) $SOCl_2$, MeOH 0 °C to reflux 3 h; (ii) p-TSA, DMAP, DMF 80 °C, overnight; (iii) NH_3(g), MeOH −40 °C to 50 °C in high pressure reactor, 6 h; (iv) $LiAlH_4$, THF, reflux, 6 h

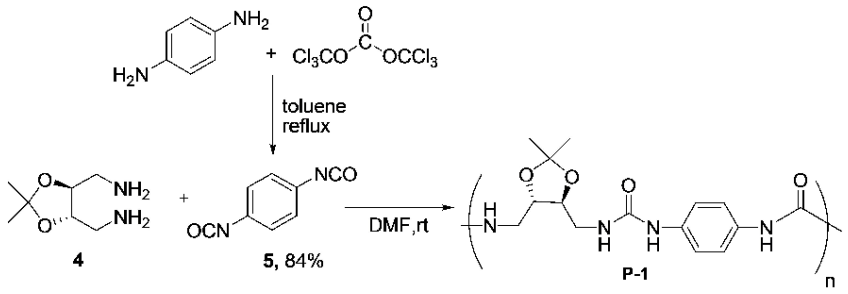

Scheme 2. Synthesis of 5 and P-1.

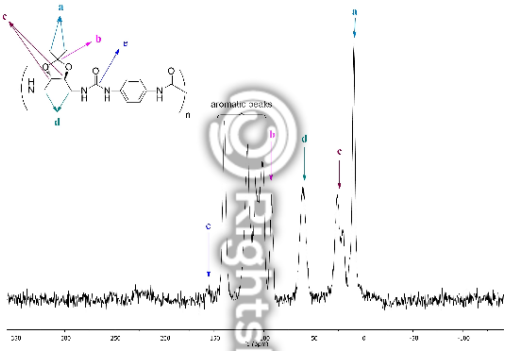

Figure 6. CP/ MASS ^{13}C NMR spectrum of P-1.

Experimentally, proving that this is a helical polymer is a daunting task due to the lack of solubility. Nevertheless, it was proposed that helicity on a single polymer chain should induce helicity at the macroscopic level due to the self-assembly. Therefore the idea was tested with Scanning Electron Microscope (SEM). The SEM images showed that there are helical segments in micrograph at macroscopic scale (Figure 7).

In the synthesis of **P-2**, to obtain helical configuration in the backbone of the polymer, *L*-lysine was chosen as a chiral monomer. *L*-lysine and triethylamine were dissolved in DMF, and 1,4- phenylene diisocyanate **5** was added onto this solution at room temperature. Polymerization was quenched by pouring reaction solution into the water, and resulting polymers were separated by filtration. (Scheme 3)

Polymer **P-2** did not dissolve in common organic solvents. For the characterization of the polymer, CP/MAS ^{13}C-NMR was also utilized. The NMR results showed that in the region between 0–90 ppm lysine carbons, labeled as **a**, appear. Aromatic carbons were in the region between 95–150 ppm. At around 160 ppm urea and carboxylic acid carbon peaks were observed. Sharp peaks might belong to DMF that can not be separated due to the hydrogen bonding (Figure 8).

The macroscopic helicity of the **P-2** was investigated with SEM, as in the case of **P-1**. However, instead of fibrous regional

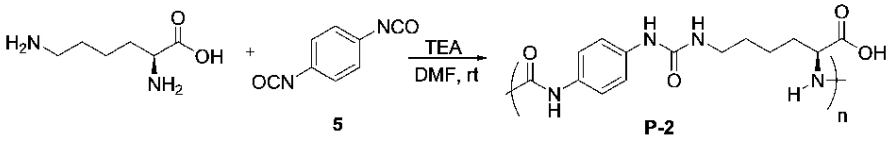

Scheme 3. Synthesis of P-2.

Figure 7. SEM image of P-1

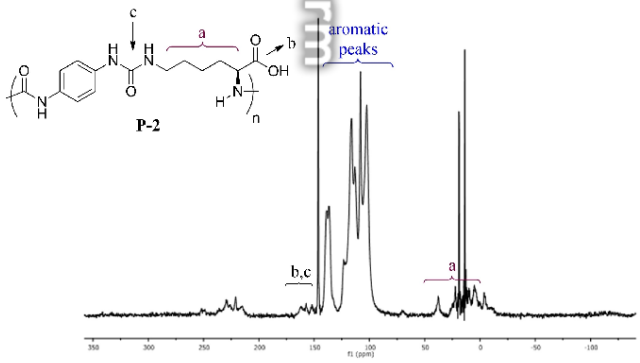

Figure 8. CP/ MASS ^{13}C NMR spectrum of P-2.

helical nanostructure formation, **P-2** formed random aggregates (Figure 9). This aggregation was caused by the long alkyl chain of lysine which has numerous conformations. The existence of these conformations could prevent the helicity of the polymer. In addition, competition of hydrogen bonds between urea-urea self interactions and between urea and lysine groups is another factor for the formation of random aggregates.

Electrostatic potential surface calculated for the optimized single **P-1** hexamer with linear initial structure have both electron deficient and electron rich parts on the urea groups as depicted for the middle part of oligomer in Figure 10a. According to this first principle calculation, 2,2-dimethyl-1,3-dioxolane structure between the (1,4-phenylene)diurea groups are relatively hydrophobic compared to highly hydrophilic urea groups in **P-1**.

Most stable structure for the hexamer modeled based on the lowest energy monomer provided by conformational analysis, demonstrated that **P-1** have helical structure as shown by experiments. These helical structures have 2 nm diameter and highly stable structures as they maintain their structures during simulations and first principle optimizations. The reason for the formation of these helical structures are mainly hydrophilic and hydrophobic interactions as demonstrated by electrostatic potential surfaces (Figure 10b and 10c). Tartaric acid based 2,2-dimethyl-1,3-dioxolane structures were placed at the center of helices and relatively hydrophilic urea groups formed outer surface of the helices. Although a different most stable packing structure was reported for pristine (1,4-phenylene)diurea hard blocks,[55] urea groups reorganized into a helical structure due to the effect of 2,2-dimethyl-1,3-dioxolane linkage. The angle formed between two urea planes owing to the 2,2-dimethyl-1,3-dioxolane self interactions in center is important for twisting of chains leading to the formation of helical structures (Figure 10c).

Equilibrium structure of the six helical **P-1** chains extracted from the equilibrium structure of 5×5 supercell of the octamers are given in Figure 10d which explain the formation

Figure 9. SEM image of P-2.

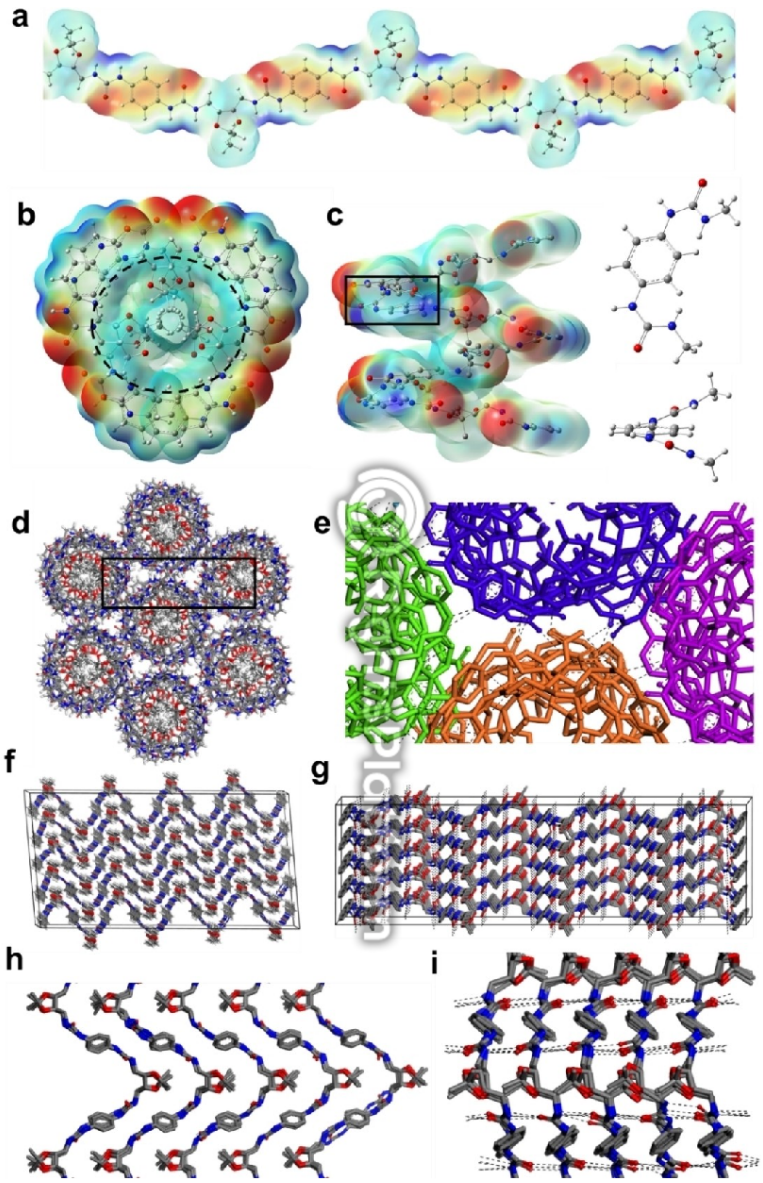

Figure 10. (a) Electrostatic potential surface of the middle part of **P-1** hexamer linear chain (Electron rich parts are in red, electron deficient parts are in blue), (b) Top view, (c) side view for the electrostatic potential surface of **P-1** helical hexamer modelled based on the lowest energy structure calculated by conformational analysis and structure of (1,4-phenylene)diurea in this helical structure, (d) Equilibrium structure of the six helical **P-1** chains taken from the 5×5 supercell of the octamers, (e) Interchain hydrogen bonds between the outer hydrophilic layer of **P-1** helical structures, (f) Equilibrium structure of the 5×5 supercell constructed by using initial linear chains from xy- and (g) xz-planes, (h) Packing motifs of the equilibrium structures constructed by using linear chains from xy- and (i) xz-planes.

of fiber like structures for **P-1**. Packing of helical **P-1** chains in the hexagonal packing resulted in the fiber like structures observed in experiments. Interhelical hydrogen bonds between ureas at the outer hydrophilic layer of **P-1** helical structures given in Figure 10e explain the stability of the fibers formed by **P-1** helices. These calculations indicate that helical structures formed intermolecular hydrogen bonding network by ureas at the surfaces of **P-1** that shape macroscale fiber formations. This microscale phase separations reflected as macroscale morphology formation due to the intersegmental interactions between hard blocks and soft blocks was previously reported for ureas and urethanes.[56,57]

Equilibrium structure of the 5×5 supercell constructed by an alternative second method where molecular dynamics simulations were performed starting from initial linear chains at low density are displayed from xy- and xz-planes in Figure 10f-10 g. Final density is reached to 1.45 g/cc which was 1.25 g/cc for hexagonal packing of **P-1** helices. Similar with the helical structure predicted by conformational analysis given in Figure 10b–e, urea groups are microphase separated from 2,2-dimethyl-1,3-dioxolane and they prefer to be in interaction with other ureas. Final wave-like packing motifs was formed as a result at the equilibrium structures given in Figure10 h–10i from two different planes. Higher number of hydrogen bonding interaction between ureas in this alternative packing structure was reflected as higher stability compared to the helical structure calculated by conformational analysis. Although this wave-like microphase separated structure that exhibit highly ordered and directional hydrogen bonds is 20–25 kcal/mol more stable per monomer compared to helical structure with less ordered and random hydrogen bonds (Figure 10i), helical structure were observed experimentally (Figure 10e). The reason behind this experimental phenomenon is mainly the solvent effect. Hydrophilic water used in experiments assists the hydrophobic 2,2-dimethyl-1,3-dioxolane move to the center and hydrophilic urea groups to the outer surface which favors the formation of helical **P-1**. However hydrophilic diurea and dimethyl-1,3-dioxolane are equally exposed at surface for the wave like structure. This means that solvent and experimental conditions are also highly important factors for the final chain behaviour of potentially helical polymers.

Calculated electrostatic potential surface for the single linear hexamer structure of **P-2** have electron deficient and electron rich parts on the urea groups as well as on the carboxylic acid group of *L*-lysine linkage given for the middle part of oligomer in Figure 11a. This is one of the main difference between **P-2** and **P-1** that *L*-lysine have hydrogen bonding capability and comparable electrostatic potential with urea, however 2,2-dimethyl-1,3-dioxolane structure between the (1,4-phenylene)diurea groups in **P-1** are relatively hydrophobic.

Most stable structure for the hexamer model based on the lowest energy monomer by using conformational analysis demonstrated that **P-2** do not have helical structure as predicted by experiments (Figure 11b). It has less ordered structure compared to **P-1** as can be explored from the end group view along the hexamer as given in Figure 11c. The origins of this disorder are intrachain hydrogen bonds between carboxylic acid group of lysine and neighboring urea group (Figure 11d) in addition to the flexibility of alkyl group. The chain is bend from the linkage between *L*-lysine and urea due to this hydrogen bond and flexible *L*-lysine. Intrachain hydrogen bonds between carboxylic acid and urea as well as ample conformational space provided alkyl chain prevented the large scale twisting of the chain and formation of helical structures in the lowest energy conformer of **P-2**.

Conformational analysis of the single chain gave us idea about the structure and morphology, still it cannot clarify the aggregation behaviour of the chains. Equilibrium structure based on the molecular dynamics simulations and minimizations by increasing cell density step by step to find lowest energy structure of supercell for **P-2** octamers is given in Figure 11e. Although the chains are aggregated and cell density reached to 1.39 g/cc, there is not any longe range order such as helical structure determined by the molecular dynamics simulations either.

This could be explained by more detailed visual analysis of equilibrium structure of this cell as given by the packing motif and corresponding hydrogen bonds of **P-2** equilibrium structures at the xy- plane given in Figure 11f and Figure 11g, respectively. This closer depiction demonstrated the presence of hydrogen bonds between carbonyl oxygen of *L*-lysine and hydrogens of urea groups in addition to the expected hydrogen bonds between ureas as reported in the literature for (1,4-phenylene)diurea aggregation.[50]

Moreover packing motif (Figure 11h) and corresponding interchain interactions (Figure 11i) for equilibrium structures of **P-2** at the xz- plane show hydrogen bonds between hydroxyl groups of *L*-lysine and carbonyl group of urea in addition to the interaction of phenyl hydrogens with carbonyl oxygen of the lysine. These multidimensional hydrogen bonds and other interactions between (1,4-phenylene)diurea and the lysine which is in competition with their self interaction of these segments caused complicated intersegmental mixing and microphase separation which leads to the random aggregation of chains in the larger scale morphologies. In summary, helical structures was not observed for **P-2** either by conformational analysis and molecular dynamics simulations.

It is determined that there is one important parameter for the formation of helical structure which is the intersegmental microphase separation between (1,4-phenylene)diurea and chiral starting material. This can be quantified by hydrophobicity, logP values calculated as −0.04, 1.41 and 0.73 for urea group, tartaric acid based 2,2-dimethyl-1,3-dioxolane and l-lysine based group, respectively. High hydrophobicity difference and weak interaction between different blocks in **P-1** leads to the formation of helical polymer in solid state. Conformational freedom, hydrogen bonding capability and self interactions of blocks are other important factors that determine formation of helical chiral polyureas.

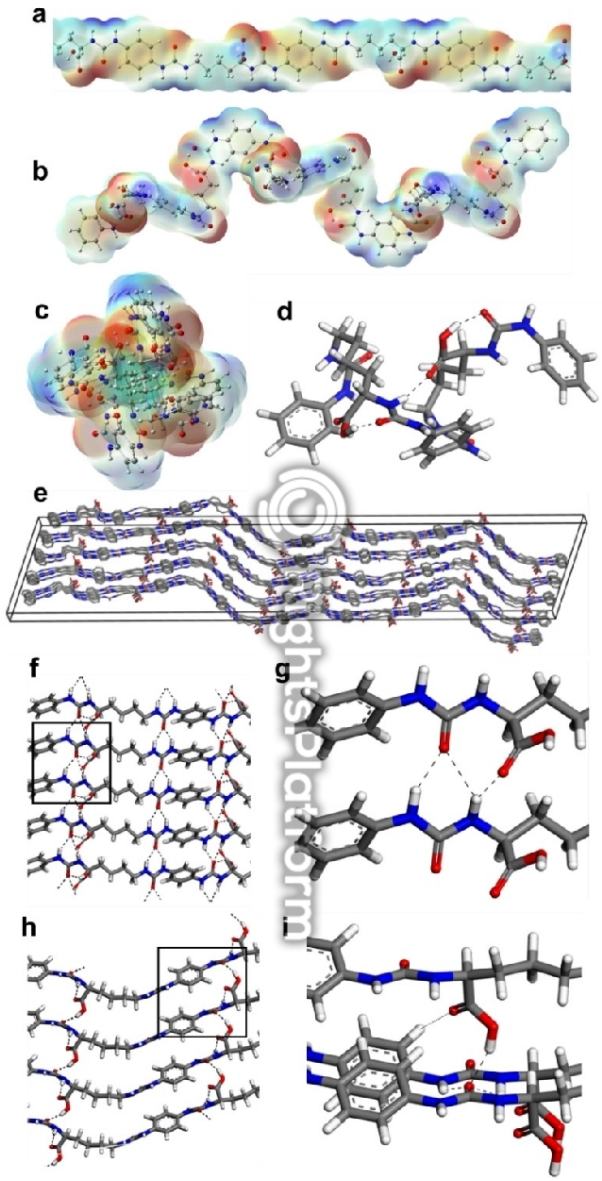

Figure 11. (a) Electrostatic potential surface of the middle part of **P-2** hexamer linear chain, (b) side view (c) top view for the electrostatic potential surface of **P-2** hexamer modelled based on the lowest energy structure calculated by conformational analysis, (d) Intrachain hydrogen bonds between carboxylic acid and urea in the lowest energy conformer of **P-2**, (e) Equilibrium structure 5×5 supercell of the **P-2** octamers based on the linear initial chains, (f) Packing motif, (g) corresponding hydrogen bonds of **P-2** equilibrium structures constructed by starting from linear initial chains at the xy- plane, (g) Packing motif and corresponding hydrogen bonds of **P-2** equilibrium structures constructed by starting from linear initial chains at the xz- plane.